Proceedings of DETC'97
1997 ASME Design Engineering Technical Conferences
September 14-17, 1997, Sacramento, California

DETC 97/DFM-4347

IMPROVING MANUFACTURING PRECISION USING THE KARHUNEN-LOÈVE TRANSFORM

Irem Y. Tumer
The University of Texas at Austin
Department of Mechanical Engineering
ETC 4.164
Austin, Texas, 78712
Phone: 512-471-7347
Email: irem@shimano.me.utexas.edu
http://shimano.me.utexas.edu/~irem

Kristin L. Wood
The University of Texas at Austin
Department of Mechanical Engineering
ETC 4.132
Austin, Texas, 78712
Phone: 512-471-0095
Email: wood@mail.utexas.edu
http://shimano.me.utexas.edu/kris.html

Ilene J. Busch-Vishniac
The University of Texas at Austin
Department of Mechanical Engineering
ETC 5.132
Austin, Texas, 78712
Phone: 512-471-3038
Email: ilenebv@mail.utexas.edu
http://www.me.utexas.edu/~microbot/IBVmain.html

ABSTRACT

The status of fault patterns on part surfaces can provide valuable information about the condition of the manufacturing system. In this work, we aim to develop a reliable fault detection and diagnosis tool in order to assure the automated production of high-quality parts. Such a tool provides a means of integrating the manufacturing and design phases. Accurate detection of the part surface condition in manufacturing ensures the fault-free design of the manufacturing parameters and machine components.

This paper introduces a mathematical transform that has the potential to detect faults in manufacturing machines. Specifically, the paper focuses on the decomposition of complex signals to allow the detection of faults. The Karhunen-Loève transform is investigated by means of numerically-generated signals. Numerical signals are studied to decompose a variety of signals, including deterministic, stochastic, stationary, and nonstationary signals. Finally, the potential utility of the proposed technique is discussed in the context of a newly-maturing manufacturing process.

IMPROVING PART PRODUCTION IN MANUFACTURING

In the era of intelligent manufacturing, it is crucial that designers and manufacturers rely on the exchange of accurate information about part production. The surface precision of a part produced during manufacturing is a crucial source of information, often not accurately known to the manufacturer or to the designer (Tumer et al., 1995; Tumer et al., 1997a; Zemel and Otto, 1996). In this work, we aim to improve and predict the part production process. Two tasks are crucial in accomplishing this goal: (1) quantifying the surface precision of parts produced from a manufacturing process; and, (2) designing/redesigning manufacturing machines and/or choosing machine parameters to produce parts with improved precision. The former is accomplished by introducing a mathematical means of detecting faults on surface profiles. The latter is accomplished by introducing a mathematical means of diagnosing the origin of these faults.

Detection of Faults for Manufacturing and Design

In this work, we aim to close the design and manufacturing loop by providing accurate information about the fault status of parts and machine components. The detection and diagnosis of faults in manufacturing systems can provide valuable information for manufacturers and designers. Manufacturers benefit from a fault-free part production, while designers benefit from an accurate isolation of design problems.

The fields of fault diagnosis and mechanical signature analysis have a significant history (Barker, 1991; Braun, 1986; Eppinger et al., 1995; Sottile and Holloway, 1994). A fault is defined as the inability of a system to perform in an acceptable manner (Eppinger et al., 1995; Sottile and Holloway, 1994). Faults typically manifest themselves as

deviations in observed behavior from a set of "normal" behaviors. In this work, faults are monitored based on signals measured from a manufacturing system, such as part surface deviations and machine tool vibrations. Fault detection is the recognition of an unacceptable behavior; and fault diagnosis is the identification of a set of parameters and/or components in the system that caused the fault.

The objective of fault detection and diagnosis is usually preventive maintenance, based on early warning of developing failures (Braun, 1986). Traditionally, preventive maintenance is used to perform regular check-ups of machine components by disassembling them when the process is shut down. Even though this method assists in accurate diagnosis of some faults, additional check-ups between these regular off-line check-ups is crucial to diagnose faults that are, for example, in the incipient stage. Incipient faults are faults that are just beginning to occur, and might lead to a serious situation in the near future. As a result, on-line quantitative diagnosis of the operation process is often required for thorough diagnosis of faults (Sottile and Holloway, 1994). This step can be very valuable for critical machinery, where an unexpected shutdown can have disastrous economical consequences. In addition, the identification of faulty components not only reduces manufacturing costs, but also often pinpoints production problems which can then be remedied. Finally, by identifying faulty patterns during manufacturing, an "undesirable" state of a system can be recognized; recognition of states such as an improper pre-loading condition of a bearing, can enable the prediction of reduced component life, even if no fault has yet developed (Braun, 1986).

To integrate the design and manufacturing phases more effectively, we propose to develop a reliable fault detection and diagnosis tool. Such a tool can be used as a means to identify parameters and components in the manufacturing machine that result in poor surface quality in final parts. Designers can use the information obtained from the proposed technique to implement simple modifications to the machine components or process parameters. Integration of detection, diagnosis, and redesign can result in potential savings in time and money. In this paper, we introduce a potential tool for this purpose and present preliminary results based on numerically generated signals. The preliminary results focus on the decomposition abilities of the proposed tool. These results are then discussed in the context of future directions with an application to a newly-maturing manufacturing process, namely, Selective Laser Sintering. The surface fault information obtained from such a tool can be potentially used to make design changes and take remedial actions.

Motivation and Current Focus

In this work, our ultimate goal is to develop a robust fault detection and diagnosis approach. Current methods of fault detection and diagnosis (e.g., Fourier transform-based methods) become problematic in the presence of nonstationarities, and other obscuring effects, resulting in false alarms or delayed warnings about the status of a manufacturing fault. Furthermore, several different methods are typically used to detect different types of patterns, whether deterministic or stochastic, implying a need for a unified method that can be used for any type of fault pattern. Finally, the current methods typically require some prior knowledge of the types of fault patterns that can be expected from a manufacturing system and base their diagnosis on this knowledge. This requirement becomes problematic when a new machine needs to be diagnosed and/or prior knowledge of the possible faults does not exist.

In an attempt to develop such an approach, we have identified two major goals which will assure robustness. The first goal is to detect and quantify a fault-indicating pattern (feature), regardless of the type and characteristics of the observed signals. The second goal is to diagnose the origin of the fault, without relying on previous knowledge or known fault patterns. To satisfy these research goals, we have proposed the following approach, shown schematically in Figure 1. The focus of this paper is on the first two steps of this approach.

- Decompose a complex manufacturing signal into decorrelated patterns in order to analyze each pattern individually.
- Monitor the decomposed patterns individually to detect the occurrence of faults.
- Quantify the severity of each pattern to determine whether it represents a significant fault on the manufactured part surface.
- Monitor submechanisms to find patterns analogous to the identified fault patterns.
- Declare a fault and determine its origin whenever an individual fault pattern compares to analogous patterns from monitored submechanisms.

One of the most crucial parts of this approach is the accurate decomposition of a complex signal into decorrelated fundamental patterns. To obtain a decorrelated decomposition of the measured signal, we need to apply a mathematical transformation to the signal (Akansu and Haddad, 1992; Whitehouse, 1994). As a result, this paper concentrates on the first two steps of our approach. To accomplish our goals, we investigate an orthogonal transform called the Karhunen-Loève (KL) transform. The KL transform decomposes signals into completely decorrelated components in the form of empirical basis functions that contain the ma-

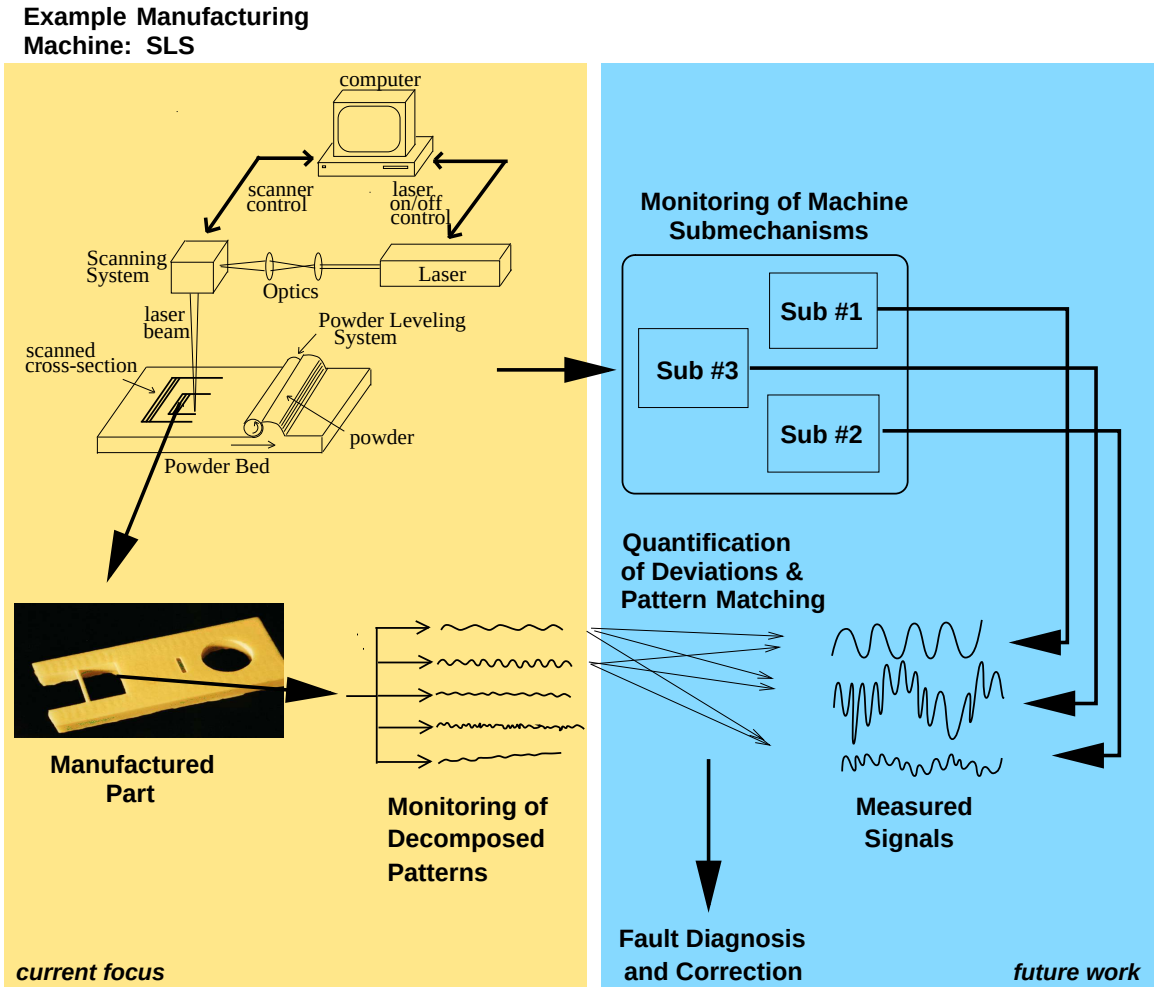

Figure 1. Fault Monitoring and Diagnosis Approach.

jority of the variations in the original data. The KL transform has not been proposed previously as a tool for fault detection and diagnosis of dynamic signals from manufacturing. The reluctance in using the transform is partially due to the difficulty in attributing physical significance to the outputs. In this paper, we show that the KL transform can be significantly extended to fault monitoring and detection. Specifically, we demonstrate the method's superior detection properties by decomposing multi-component signals into decorrelated fault patterns. These fundamental patterns are promising candidates to determine fault occurrence. The mathematical foundations of the the extension to the KL transform for use in monitoring and detection of fault patterns are presented in a subsequent paper (Tumer et al., 1997b). Future work will focus on the ability of the proposed method to diagnose the origin of the identified fault mechanisms.

THE KARHUNEN-LOÈVE TRANSFORM

The Karhunen-Loève (KL) transform is studied in this work because of its inherent ability to obtain an accurate decomposition of signals into dominant individual components. The power of the KL transform stems from the fact that it can be applied to any type of signal, whether deterministic, stochastic, stationary, or nonstationary, without prior knowledge of the characteristics of the fault patterns (Fukunaga, 1972; Kozek, 1993; Therrien, 1992; Tumer et al., 1997b). Nonstationarities are patterns with time-varying statistics, which become problematic when using Fourier-based methods. Stochastic nonstationary signals are typically modeled as a set of deterministic functions operating on otherwise stationary stochastic components (Bendat and Piersol, 1986; Tumer et al., 1997b). Methods that perform a time-averaging operation result in the masking of nonstationary features, which of-

ten appear incorrectly as a low-frequency sinusoidal component (Tumer et al., 1995; Tumer et al., 1997b). The KL method presents us with the ability to work with nonstationary signals (Fukunaga, 1972; Kozek, 1993; Therrien, 1992; Tumer et al., 1997b). In addition, high variability stochastic components often obscure the coherent data and result in a low signal-to-noise ratio. The KL method acts as a filter which increases the signal-to-noise ratio; the dominant components correspond to the important features, whereas the low-significance components contain the variability in the data. Reconstruction of estimates of the original data have increased signal-to-noise ratios when the low-significance components are omitted.

The Karhunen-Loève transform is used in a variety of signal processing applications (Akansu and Haddad, 1992; Algazi et al., 1993; Ball et al., 1991; Fukunaga, 1972; Therrien, 1992; Sirovich and Keefe, 1987; Zahorian and Rothenberg, 1981). However, applications of the KL transform in the fault detection and diagnosis of manufacturing signals are nonexistent. The transform has been used in statistical and pattern recognition fields to decompose the data into its principal components and reconstruct the original data with reduced dimensionality. However, typically, attributing physical significance to these empirical eigenfunctions is not trivial. We claim that, when the transform is applied to signals from manufactured surfaces, the resulting dominant patterns correspond to coherent mechanisms in the measured signal and can be monitored individually to detect any deviations from the normal state of operation of the manufacturing machine, hence indicating faults. Furthermore, we claim that the decomposition is accurate and is valid in the presence of stochastic components, as well as nonstationarities. In this light, the following is a detailed study of the outputs and the decomposition properties of the KL transform, based on numerically-generated signals. The analytical derivation of the KL outputs to understand the decomposition properties is presented in a subsequent paper (Tumer et al., 1997b).

Mathematical Basis for Simulations

In the context of surface profile characterization, the signal being monitored is the surface profile of a part being manufactured. A total of M "snapshots" are assumed to be collected at regular intervals to allow for a continual monitoring of the state of operation. Each snapshot has a total of N sample points.

The collected snapshot profile measurements are the $\vec{P}_m$ input vectors for the KL analysis. First, the mean vector $\vec{P}_{ave} = \frac{1}{M}\sum^m \vec{P}_m$ over all M samples in the ensemble is computed; then the deviation or departure $\vec{d}_m = \vec{P}_m - \vec{P}_{ave}$ of each sample signal from the ensemble mean is computed. Next, using the deviations of the input snapshots from the mean profile, the covariance matrix is computed as follows:

$$\vec{V} = \frac{1}{M}\sum_{m=1}^{M} \vec{d}_m[\vec{d}_m]^T, \tag{1}$$

where M is the number of input vectors for the method, or snapshots of the process being monitored. The covariance matrix contains all the variation in the input data. Then, the eigenvalues and eigenvectors of the covariance matrix are computed. The eigenvectors of $\vec{V}$ are the basis functions $\vec{e}_i$ which satisfy the following eigenvector equation:

$$\vec{V}\vec{e}_i = \lambda_i \vec{e}_i \tag{2}$$

The eigenvalues λ_i are then ordered, and the relevant features are selected by choosing the first $n < N$ dominant eigenvalues from the set of solutions, based on a feature selection criterion; 90% of the total energy is sufficient for reconstruction (Ball et al., 1991). Each original sample deviation vector can then be reconstructed with reduced dimensionality $n < N$ using:

$$\vec{d} = \sum_{i=1}^{n} c_i \vec{e}_i \tag{3}$$

where the coefficients c_i are computed by projecting each sample vector deviation $\vec{d}_m$ onto the basis vectors $\vec{e}_i$ from:

$$c_i = [\vec{d}_m]^T \vec{e}_i. \tag{4}$$

These coefficients represent the original data in the new domain represented by the dominant eigenvectors (basis functions). Each original sample vector $\vec{P}_m$ is then reconstructed with lower dimensionality by adding this linear combination to the sample mean:

$$\vec{P}_m = \vec{P}_{ave} + \sum_{i=1}^{n} c_i \vec{e}_i \tag{5}$$

SIMULATING FAULTS DURING MANUFACTURING

In this work, we claim that the eigenvectors computed from the covariance matrix represent the fundamental shapes of the individual faults patterns. Once we decompose the measured signal into decorrelated fault patterns,

the significance of each fault pattern is determined by its energy content. The individual energy content is indicated by the ratio of the corresponding eigenvalue to the sum of all eigenvalues. We then claim that any change in the fundamental fault patterns is indicated by the corresponding coefficient vector. The coefficient vector represents the weight of a fundamental shape in each snapshot collected over time.

In order to test the suitability and limitations of the KL transform, we use analytical signals in which the fault patterns are known. This assures the accuracy of our results, since we know the exact characteristics and shape of each fault pattern, and we know exactly when each type of fault pattern occurs. We develop a series of analytical signals for two purposes: to model multicomponent signals to show the types of fault patterns that can be detected with this technique; and to model the occurrence of faults during a normal state of operation in order to show that the KL transform can be used to detect faults when they occur. Multicomponent signals are defined to be signals consisting of a combination of patterns, as opposed to "pure" signals consisting of a single signal pattern.

Analytical Signals

We simulate cases where different faults occur during a manufacturing process, and compare these cases to a "normal" state of operation of the manufacturing process. Deterministic and stationary changes are introduced, as well as nonstationary changes over the entire profile and over each individual snapshot.

The "normal" state of operation is assumed to produce a multicomponent signal with 2 sinusoids, in the form of $A_1 sin(F_1 j) + A_2 sin(F_2 j)$: one high frequency ($F_1 = 0.9\ rad/sec$), small amplitude ($A_1 = 1\ mm$), and the other low frequency ($F_2 = 0.2\ rad/sec$) and large amplitude ($A_2 = 2\ mm$), plus random (Gaussian) noise (zero mean and variance of 0.09). This situation illustrates a typical operation state, in which rotating components introduce fundamental sinusoidal patterns, accompanied with random noise from the machine operation or other conditions. Faults, such as bearing wear or misalignment, introduce either additional harmonics, or a change in the magnitude of the fundamental frequency components. In addition, offsets or linear trends may be introduced as a result of misalignment in the non-rotating elements.

In the first set of deviations from this normal state of operation, stationary changes are introduced over the snapshots. Ten snapshots are assumed to be collected over the entire profile; each snapshot has 256 sample points. The second set of simulations tests the effect of introducing sudden and/or gradual nonstationary changes to the monitored signal. These cases simulate the occurrence of faults after a certain point in time, introducing a nonstationary pattern over the monitored signal. The following cases are simulated and compared to the normal state of operation:

1. The high frequency component increases in amplitude, the remaining patterns are the same as the normal state of operation; two different amplitude values are simulated (Faulty States 1a and 1b).
2. The mean offset of the normal state of operation changes while monitoring the signal, introducing a nonstationary pattern: the first ten snapshots collected have the same components as the normal state of operation, while the next ten snapshots have an offset value added (Faulty State 2).
3. The amplitude of the low frequency component increases while monitoring the signal, introducing a nonstationary pattern: the first ten snapshots are the normal state of operation, while the next ten snapshots have a change in the magnitude of the low frequency component (Faulty State 3).
4. The normal state of operation is modified by a linear trend added over the entire profile from which ten snapshots are collected, introducing a nonstationary pattern (Faulty State 4).

Simulation Results

Table 1 presents the eigenvalues (Equation 2) for the normal state of operation, the set of simulations with stationary changes, and the set of simulations with nonstationary changes over the snapshots. Note that the eigenvalues correspond to the mean-squared value of the coefficient vectors. The significance of each pattern is indicated by the magnitude of the eigenvalues. A change in the severity of a particular pattern can be indicated by a corresponding change in the significance of the eigenvalues. The significance of the resulting eigenvalues in Table 1 will be discussed in the following subsections. Notice that the eigenvalues are always listed in a descending order. Thus one cannot assume that the index i corresponds to the same eigenvector in each case. Any differences are explained in each case.

Normal State of Operation The normal state of operation consists of multi-component snapshots with two sinusoidal components and random noise. The eigenvectors are computed using Equation 2 and the coefficient vectors are computed using Equation 4. The dominant eigenvectors are shown in Figure 2a and 2b, and the corresponding coefficient vectors are shown in Figure 2c and 2d.

We first observe that, for the normal state of operation,

Table 1. Eigenvalues: Normal State vs. Faulty States.

Index	Normal	Faulty 1a	Faulty 1b	Faulty 2	Faulty 3	Faulty 4
1	255.45	633.47	6938.42	1602.78	3243.81	346191.37
2	240.15	530.83	5738.31	254.08	3191.27	254.37
3	74.01	240.76	245.89	239.45	71.59	240.01
4	55.62	235.70	235.65	69.86	56.26	69.38
5	2.68	2.81	2.86	55.23	1.52	56.66
6	2.58	2.39	2.62	1.66	1.49	2.36
7	2.25	2.25	2.39	1.41	1.36	2.21
8	2.14	2.00	2.06	1.32	1.33	2.11
9	2.00	1.73	1.79	1.24	1.26	1.92
10	0.00	0.00	0.00	1.22	1.22	0.03

the multi-component signal is decomposed into 4 significant eigenvalues, shown in Table 1, summing to 98% of the total energy in the signal. The first two eigenvalues (#1,#2) correspond to low-frequency sinusoidal eigenprofiles, while the next two eigenvalues (#3,#4) correspond to high-frequency sinusoidal eigenprofiles. We first notice that we have two sets of eigenvectors/eigenvalues per frequency component. This result is due to the way the original snapshot data is generated: a long sequence of data (representing the signal being monitored) is divided into M shorter subsequences (representing the snapshots collected at regular intervals for condition monitoring), which results in snapshots of sinusoids with randomly varying phase angles. As a result, the phase is detected as a separate feature in the KL decomposition. This can be seen in Figure 2a, where eigenvectors #1 and #2 are offset by a phase difference only.

This result is verified using pure sinusoid input snapshots. When only the amplitudes of the sinusoids are varied from one snapshot to the other (fixed frequency, fixed phase), the KL transform results in a single eigenvector corresponding to the fixed frequency (Figure 3a). If the same simulation is carried out using pure sinusoids with varying phase angles (fixed frequency), the KL transform results in a pair of eigenvectors, same frequency, different phase (Figure 3b). On the other hand, if the snapshots for the KL transform have a fixed phase angle, but varying frequency, we extract features corresponding to the different frequency values. The eigenvalues for the different cases run using a pure sinusoid are shown in Table 2. Ten snapshots are used for each case: Case 1 corresponds to the case with a pure sinusoid, with fixed frequency and amplitude, but varying phase angle; Case 2 corresponds to the case with fixed phase and frequency, but varying amplitude; Case 3 corresponds to the case where the amplitude and phase of the snapshots are fixed, but the frequency varies.

Table 2. Eigenvalues for a Pure Sinusoid

Index	Case 1	Case 2	Case 3
1	312.107697	10.576263	12.843555
2	149.827148	0.000001	12.685099
3	0.000038	0.000001	12.566921
4	0.000018	0.000000	12.566634
5	0.000011	0.000000	12.566548

Stationary Faults: Faulty States 1a and 1b Our first example of a fault situation deals with changes in amplitudes due to a fault in the system. In this case, the high frequency sinusoidal component of the signal increases in magnitude, while the second sinusoidal component remains unchanged. Faulty states 1a and 1b represent two different magnitudes. They can be used to determine whether changes in the amplitude of one of the sinusoidal components of the multi-component signal can be detected with the KL transform.

The eigenvalues from faulty states 1a and 1b, compared to the normal state, are shown in Table 1. As in the case of the normal state of operation, for faulty states 1a and 1b, we obtain 4 principal eigenvalues and eigenprofiles. When we increase the magnitude of the high-frequency component of the input signal, we notice that the eigenvalues corresponding to the high-frequency component increase in magnitude (Eigenvalues #1 and #2, Faulty 1a and 1b, Table 1), compared to the corresponding eigenvalues in the normal state of operation (Eigenvalues #3 and #4, Normal, Table 1). Notice that the magnitude of the eigenvalues for Faulty states 1a and 1b reflect the increase in the magnitude of the high-frequency sinusoidal component. The eigenvalues corresponding to the low-frequency component (Eigenvalues #3 and #4, Faulty 1a and 1b, Table 1) remain ap-

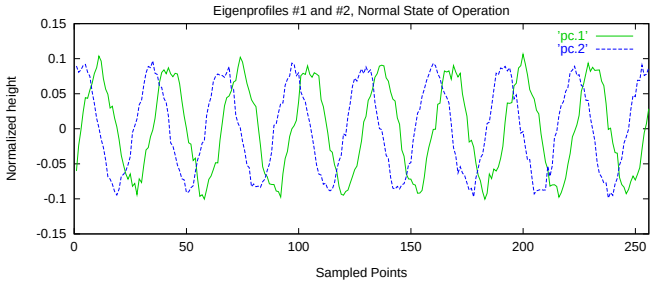

(a) Eigenvectors #1 and #2 (low frequency).

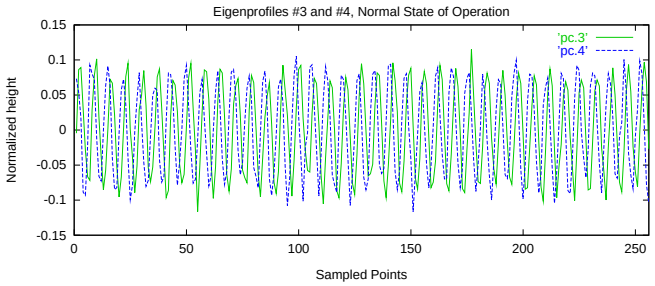

(b) Eigenvectors #3 and #4 (high frequency).

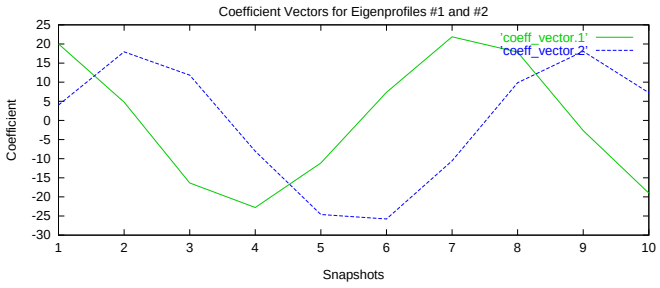

(c) Coefficient Vectors #1 and #2.

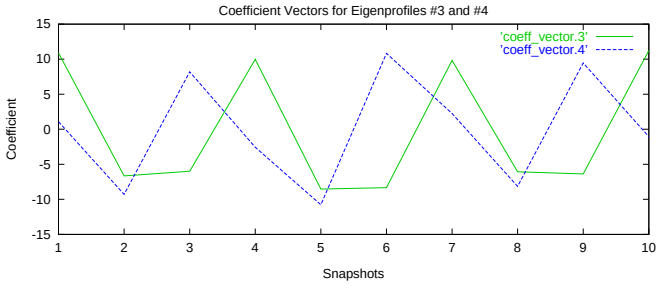

(d) Coefficient Vectors #3 and #4.

Figure 2. Normal State of Operation.

proximately the same as in the normal state of operation (Eigenvalues #1 and #2, Normal, Table 1).

These trends are more easily noticeable when we study the shape of the eigenprofiles and the corresponding coefficient vectors. The main two eigenvectors from faulty states 1a and 1b, and the corresponding coefficient vectors, compared to the normal state, are shown in Figure 4. Notice that the shape of the eigenprofiles are approximately the same for the normal state, and faulty states 1a and 1b (Figures 4a and 4b). This result is expected since we are only changing the magnitude of the high-frequency sinusoidal component, and not the frequency. The change in magnitude is detected using the coefficient vectors. Also notice that the coefficient vectors corresponding to the high-frequency component show a steady increase in magnitude (Figure 4c). On the other hand, the coefficient vectors corresponding to the low-frequency component show no detectable change. The change in magnitude is successfully detected by monitoring the coefficient vectors (Figure 4d).

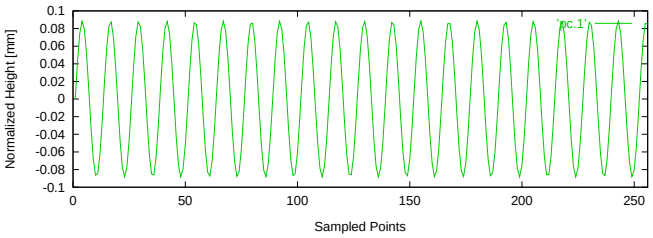

(a) Varying Amplitude, Fixed Frequency & Phase.

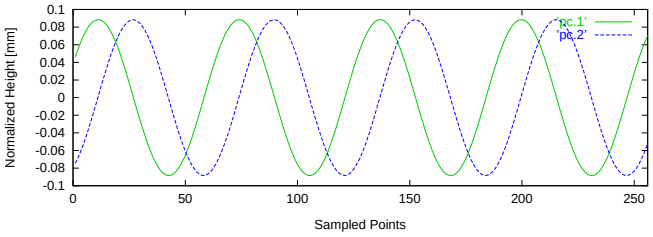

(b) Varying Phase, Fixed Frequency & Amplitude.

Figure 3. Eigenvectors for a Pure Sinusoid.

Nonstationary Faults: Faulty State 2 Our next fault situation deals with the introduction of sudden nonstationary changes to the monitored signal. In this case, signals from the normal state of operation are assumed to have a sudden change in the mean offset level of the monitored signal. The nonstationary change in the signal must be detected during monitoring. In the simulations, the first ten snapshots indicate normal status, while the next ten snapshots indicate an offset change.

As shown in Table 1, this fault manifests itself as an added principal eigenprofile, with a relatively large eigenvalue (Eigenvalue #1); the remaining eigenvalues are approximately the same as the normal state of operation (Eigenvalues #2 and #3 in the faulty state 2 compare to eigenvalues #1 and #2 in the normal state, etc.). The simulation results, shown graphically in Figure 5a, show that

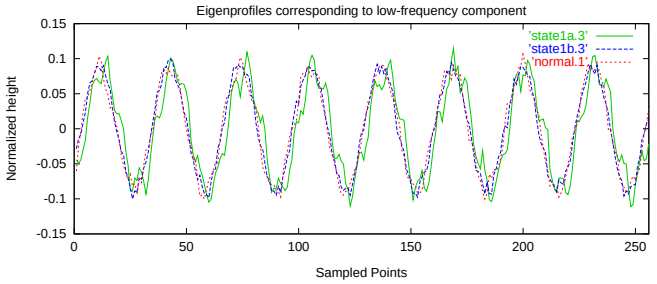

(a) Eigenvectors #1 and #2 (low frequency).

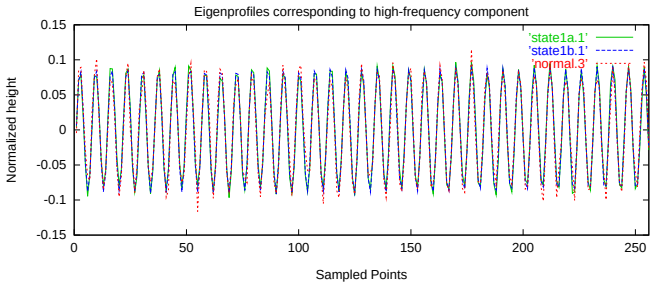

(b) Eigenvectors #3 and #4 (high frequency).

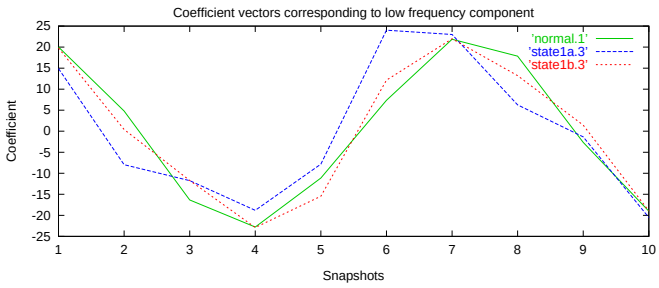

(c) Coefficient Vectors #1 and #2.

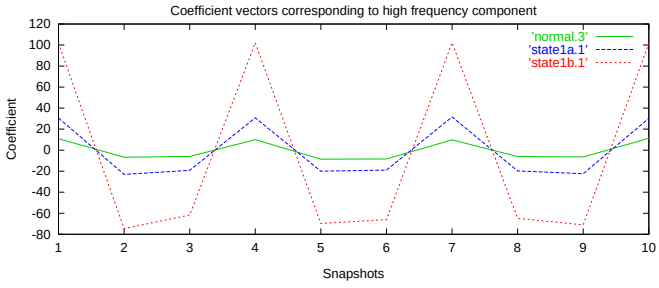

(d) Coefficient Vectors #3 and #4.

Figure 4. Normal vs. Faulty States 1a & 1b.

the first eigenprofile resembles a straight line when plotted with the remaining sinusoidal eigenprofiles. In addition, the coefficient vector corresponding to the first eigenvalue shows the change in the mean offset very clearly, after the tenth snapshot (Figure 5b). As a result, this additional pattern, defined by a straight line, can be detected by monitoring the occurrence of a fifth eigenprofile, while its significance can be evaluated by monitoring the shape of the coefficient vector. Note that no change is observed in the remaining eigenprofiles or coefficient vectors, when compared with the normal state of operation.

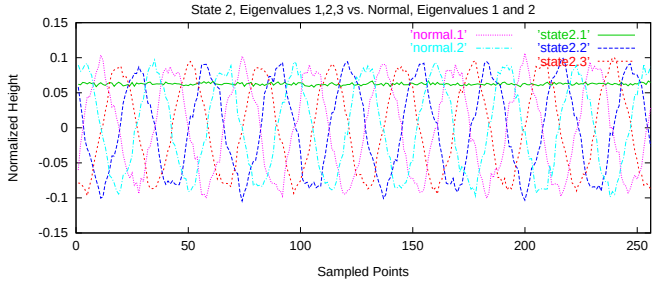

(a) Eigenvectors #1, #2, and #3.

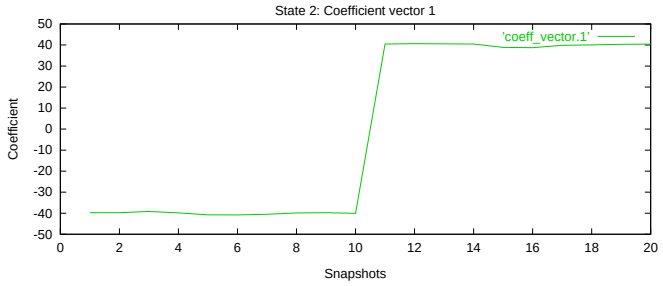

(b) Coefficient Vector #1.

Figure 5. Principal Eigenprofiles and Coefficient Vector for Faulty State 2.

Nonstationary Faults: Faulty State 3 Our third example illustrates a nonstationary change in the magnitude. In this case, the low-frequency sinusoidal component suddenly undergoes a change in magnitude, while the high-frequency component remains the same. We collect a total of twenty snapshots; a change occurs during the course of monitoring the signal, hence introducing a nonstationary change in the signal, after the tenth snapshot. The results show that, while the eigenprofiles remain the same as in the normal state of operation, the coefficient vectors corresponding to the low-frequency eigenprofiles increase in magnitude after the tenth snapshot, where the nonstationary change occurs (Figure 6a). As expected, no change is observed in the high-frequency coefficient vectors (Figure 6b). Also notice the increase in the eigenvalues for the first two eigenprofiles with respect to the normal state of operation, while the eigenvalues for the next two eigenprofiles are approximately

the same as in the normal state of operation, as shown in Table 1.

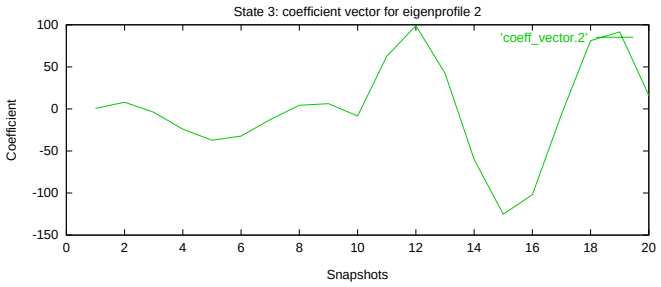

(a) Coefficient Vector #1 (low frequency).

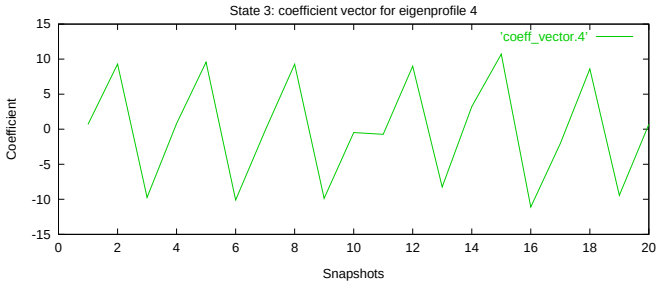

(b) Coefficient Vector #3 (high frequency).

Figure 6. Coefficient Vectors for Fault State 3.

Nonstationary Faults: Faulty State 4 In the final case, the normal state of operation is interrupted by the addition of a linear trend with a positive slope. The results show the addition of a fifth eigenvalue (Eigenvalue #1, Table 1) of large magnitude, indicating a severe fault pattern, while the remaining four eigenvalues (#2 − #5) are approximately the same as the normal state of operation. The first three eigenprofiles are shown in Figure 7a, and the coefficient vector corresponding to the first eigenprofile are shown in Figure 7b. As expected, the first eigenprofile represents a straight line as the basis vector, while the corresponding coefficient vector indicates the change in the magnitude of that principal eigenprofile, reflecting the slope in the linear trend.

Conclusions from the Simulation Results The simulation results show that the KL transform has a good potential for detecting, extracting, and monitoring fault patterns on surface profiles. First, the KL transform successfully decomposes the multi-component signal into its fundamental patterns (eigenprofiles). Changes in these fundamental patterns are successfully reflected in the corresponding coefficient vectors. The introduction of additional patterns are also detected as additional fundamental patterns. For example, for the faulty state 2, the KL transform successfully decomposes the signal into its individual patterns, i.e., 2 sinusoids and a straight line. Monitoring is done by detecting a fifth eigenprofile and studying the change in the corresponding coefficient vector. In addition, the nonstationary change in the offset level is reflected in the relevant coefficient vector, hence allowing the effective monitoring of this nonstationary change in the normal state of operation. In faulty state 3, the sudden change in the magnitude of the sinusoidal patterns is successfully reflected in the relevant coefficient vectors, while no additional patterns are extracted. In faulty state 4, the KL transform extracts the additional fundamental pattern, represented as a straight line, and detects the introduction of a linear trend, which is reflected in the corresponding coefficient vectors as a linear increase in magnitude over the set of snapshots.

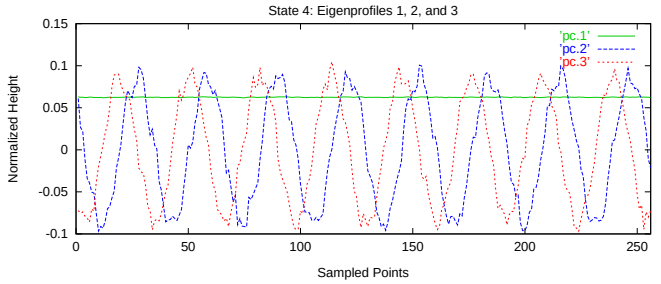

(a) Eigenvectors #1, #2, and #3.

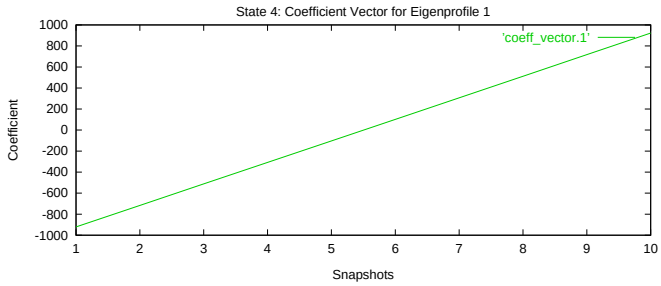

(b) Coefficient Vector #1.

Figure 7. Principal Eigenprofiles and Coefficient Vectors for Faulty State 4.

FUTURE DIRECTIONS FOR INTEGRATED DESIGN IN MANUFACTURING

The work presented in this paper has the potential to provide a valuable tool for integrating the design and manufacturing fields. In this section, future directions with a real-world application are discussed in the context of a

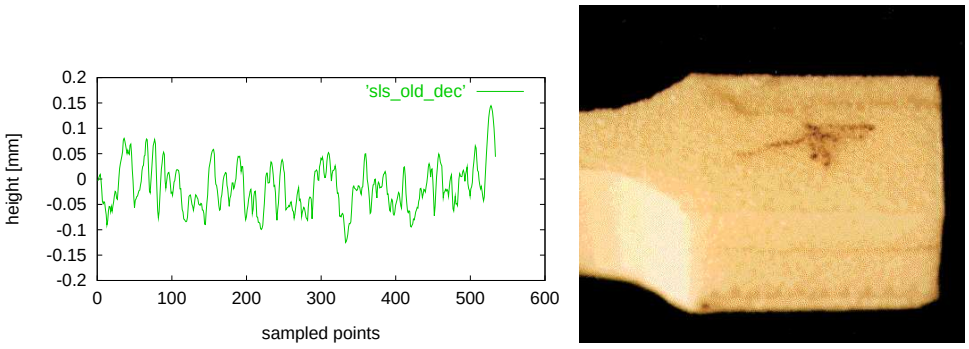

(a) SLS Part Surface, Polycarbonate #1.

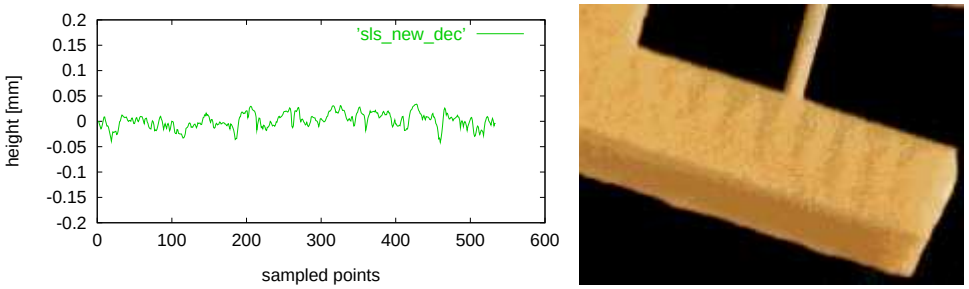

(b) SLS Part Surface, Polycarbonate #2.

Figure 8. Fault Patterns on Selective Laser Sintering Parts.

newly maturing manufacturing process, namely, Selective Laser Sintering (SLS). SLS is a layered manufacturing process in which a multitude of mechanisms interact to produce the final parts. The part is produced in steps by scanning a preprogrammed cross-section onto a layer of powder with a laser beam. A piston/actuator mechanism is used to deliver powder to the bed surface; a roller mechanism is used to spread the fresh layer of powder evenly on the bed surface; and a laser/galvanometer mechanism is used to scan the pre-determined shape of the final part for each layer (Tumer et al., 1997a). Each of these submechanisms, as well as their interactions, are potential sources of faults on SLS parts.

Let us briefly study a possible design scenario. Consider the production of SLS parts using polycarbonate powder as the raw material. The decisions involved in the production of high-quality parts are illustrated here briefly. In a previous paper, the authors have shown that, polycarbonate powder material used in a typical SLS part production results in parts with a very rough surface finish (Tumer et al., 1997a). An experimental part using such a polycarbonate material is shown in Figure 8a, along with a typical surface profile. The surface profile has an average surface roughness of $30\mu m$, which approximately corresponds to the particle diameter used for this part. The profile also shows an average vertical range of $270\mu m$, which is of unacceptable quality. A Fourier analysis of the surface, as well as a Karhunen-Loève decomposition of the surface profiles, indicate a stochastic fault pattern, which is dominated by the powder particle distribution. The RMS value of the stochastic surface profile is analogous to the particle size (Tumer et al., 1997a). The resulting remedial action is to improve the surface quality by switching to an alternative polycarbonate powder, with a smaller particle size. No other fault information is obtainable from these parts.

Figure 8b shows a part produced with the alternate powder, along with a measurement of the surface profile (Tumer et al., 1997a). The surfaces from these experiments are much less rough, with an average roughness of $10\mu m$ and an average vertical range of about $80\mu m$. Clearly, the remedial action for the designer has resulted in improved surface finish, which is deemed satisfactory by the designers for their application. However, a Karhunen-Loève analysis of the parts built using the alternative powder material reveal additional fault patterns. Figure 9 shows the fundamental KL patterns found from longitudinal measurements of the surface of such a part. The deterministic pattern in Figure 9 is indicative of machine faults which need to be remedied. Preliminary vibrational measurements from different machine components indicate a periodic pattern gen-

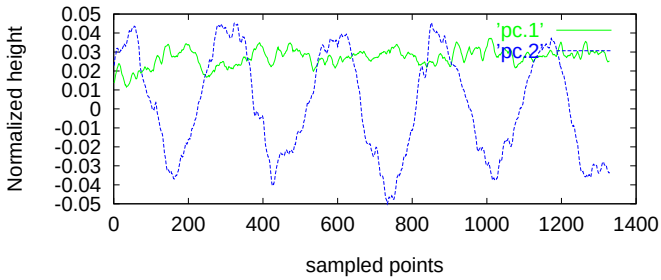

Figure 9. Fundamental KL Patterns on Selective Laser Sintering Parts.

erated by the roller motion. The period of the KL pattern roughly corresponds to the period of the vibrational patterns measured from the roller. The stochastic component indicated in Figure 9 may be due to the particle size. Further analysis of this pattern is required. The results from the KL analysis can be used to determine the severity of the fundamental modes. Design changes such as roller redesign and/or scanning parameter re-adjustments will follow diagnosis of such faults. Future work is on the way to study such diagnostic design changes.

CONCLUSIONS

This paper presents a promising tool to assure reliable information exchange about the fault status of manufacturing machines. An alternative fault detection and diagnosis tool based on the Karhunen-Loève (KL) transform is introduced. The KL transform is shown to have superior decomposition properties, which is a crucial step in fault detection and diagnosis. Multicomponent signals simulating stationary and nonstationary fault signals from manufacturing machines are decomposed into decorrelated fundamental fault patterns (eigenvectors). The status of potential fault patterns is monitored by means of corresponding coefficient vectors and eigenvalues.

The KL transform is then discussed in the context of future directions to integrate the design and manufacturing fields. The information obtained from reliable fault detection and diagnosis tools will be crucial in designing and/or redesigning the SLS machine and/or choosing process parameters such as material type. The method presented in this paper has great potential in accomplishing the task of producing accurate parts on a repeatable basis. The mathematical basis of the proposed method is being investigated thoroughly (Tumer et al., 1997b). Furthermore, experiments are being planned to show the validity of the method in real-world applications.

ACKNOWLEDGEMENT

This material is based on work supported, in part, by The National Science Foundation, Grant No. DDM-9111372; an NSF Young Investigator Award; by a research grant from TARP; plus research grants from Ford Motor Company, Texas Instruments, and Desktop Manufacturing Inc., and the June and Gene Gillis Endowed Faculty Fellowship in Manufacturing.

REFERENCES

Akansu, A. and Haddad, R., 1992. *Multiresolution Signal Decomposition: Transforms, Subbands, Wavelets.* Academic Press, Inc., San Diego, Ca.

Algazi, V. R., Brown, K. L., and Ready, M. J., 1993. Transform representation of the spectra of acoustic speech segments with applications, part I: General approach and application to speech recognition. *IEEE Transactions on Speech and Audio Processing*, 1(2):180–195.

Ball, K., Sirovich, L., and Keefe, L., 1991. Dynamical eigenfunction decomposition of turbulent channel flow. *International Journal for Numerical Methods in Fluids*, 12:585–604.

Barker, R. W., 1991. *Incipient Fault Detection Using Higher-Order Statistics.* PhD thesis, The University of Texas, Austin, Tx.

Bendat, J. S. and Piersol, A. G., 1986. *Random Data: Analysis and Measurement Procedures.* John Wiley & Sons, New York, NY.

Braun, S., 1986. *Mechanical Signature Analysis: Theory and Applications.* Academic Press, London.

Eppinger, S. D., Huber, C. D., and Pham, V. H., 1995. A methodology for manufacturing process signature analysis. *Journal of Manufacturing Systems*, 14(1):20–34.

Fukunaga, K., 1972. *Introduction to Statistical Pattern Recognition.* Academic Press, New York, NY.

Kozek, W., 1993. Matched generalized gabor expansion of nonstationary processes. In *The Twenty Seventh Asilomar Conference on Signals, Systems, & Computers*,

volume 1, pages 499–503.

Sirovich, L. and Keefe, L., 1987. Low-dimensional procedure for the characterization of human faces. *Journal of the Optical Society of America*, 4(3):519–524.

Sottile, J. and Holloway, L. E., 1994. An overview of fault monitoring and diagnosis in mining equipment. *IEEE Transactions on Industry Applications*, 30(5):1326–1332.

Therrien, C., 1992. *Discrete Random Signals and Statistical Signal Processing*. Prentice Hall, Englewood Cliffs, NJ.

Tumer, I., Srinivasan, R., and Wood, K., 1995. Investigation of characteristic measures for the analysis and synthesis of precision-machined surfaces. *Journal of Manufacturing Systems*, 14(5):378–392.

Tumer, I., Thompson, D., Wood, K., and Crawford, R., 1997a. Characterization of surface fault patterns with application to a layered manufacturing process. *Accepted for publication in the Journal of Manufacturing Systems*.

Tumer, I., Wood, K., and Busch-Vishniac, I., 1997b. Monitoring fault condition during manufacturing using the Karhunen-Loève transform. In *1997 ASME Mechanical Vibration and Noise Conference, System Health Monitoring Symposium*, Sacramento, California.

Whitehouse, D., 1994. *Handbook of Surface Metrology*. Institute of Physics Publishing, Bristol, UK.

Zahorian, S. A. and Rothenberg, M., 1981. Principal-components analysis for low-redundancy encoding of speech spectra. *Journal of the Acoustical Society of America*, 69(3):519–524.

Zemel, M. and Otto, K., 1996. Use of injection molding simulation to assess critical dimensions and assign tolerances. In *The 1996 ASME Design Engineering Technical Conference and Computers in Engineering Conference*, volume DFM-1277.